Density-functional bridge between surfaces and interfaces

B. I. Lundqvist, A. Bogicevic (1), K. Carling, S.V. Dudiy, S. Gao, J. Hartford (2), P. Hyldgaard, N. Jacobson, D. C. Langreth (3), N. Lorente (4), S. Ovesson, B. Razaznejad, C. Ruberto, H. Rydberg, E. Schröder, S.I. Simak, G. Wahnström, and Y. Yourdshahyan (5)

Department of Applied Physics, Chalmers University of Technology and Göteborg University, SE-412 96 Göteborg, Sweden,

(1) Chemistry Department, Ford Research Laboratory, MD 3083 SRL, Dearborn, MI 48121-2053, USA,

(2) COMBRA AB, Turebergsvägen 3, S-191 47 Sollentuna, Sweden,

(3) Department of Physics and Astronomy, Rutgers University, Piscataway, New Jersey 08854-8019, USA,

(4) Laboratoire Collisions, Agrégats, Réactivité, IRSAMC, Université Paul Sabatier, 118 route de Narbonne, 31062 Toulouse, cedex France,

(5) Department of Chemistry and Laboratory for Research on the Structure of Matter, University of Pennsylvania, Philadelphia, PA 19104-6323 USA.

(February 7, 2001)

Abstract

Interfaces are brought into focus by many materials phenomena, *e.g.*, contacting, materials strength, and wetting. The class of interfaces includes ultra-high-vacuum surfaces, which provide a meeting place for numerous accurate experimental techniques and advanced theory. Such meetings stimulate detailed comparisons on the quantum level between experiment and theory, which develop our theoretical tools and understanding. This creates good po-

sitions for broadened applications, *e.g.*, other interfaces, which typically lack adequate experimental tools. Density-functional theory is one key bridge between surfaces and other interfaces. The paper presents some recent typical applications from our group, including brief reports on interface structures (VN/Fe, TiC/Co, TiC/Al_2O_3), dynamic processes at surfaces and interfaces (O_2/Al(111), STM spectroscopy and manipulation), adsorption and desorption (CO,N_2,NO, and O_2 on Al(111)), electronic and magnetic properties at surfaces and interfaces (magnetic effects on TiC/Co, surface state on κ-$Al_2O_3(00\overline{1})$), and epitaxial growth on surfaces (Al(111) and alike). Similar progress in many world-wide materials groups and networks gives a basis for the ongoing paradigm shift in materials science.

I. INTRODUCTION

The scope of this international symposium is to bring together recent advances in experimental and theoretical approaches of surfaces and interfaces as different symmetry crossing. We have tried to take this purpose seriously and will illustrate this approach with some recent results from our Materials- and Surface-Theory group. Several of the topics of the symposium will be touched upon, including surface and interface structures (our examples: VN/Fe, TiC/Co, TiC/Al_2O_3), dynamic processes at surfaces and interfaces (O_2/Al(111)), adsorption, desorption (CO,N_2,NO,O_2/Al(111)), and atomic-scale manipulation, electronic and magnetic properties at surfaces and interfaces (κ-$Al_2O_3(00\overline{1})$, TiC/Co), and epitaxial growth on surfaces (Al(111) and alike). Some of the theses of this paper are (1) surfaces provide platforms to sharpen our theoretical tools, thanks to a multitude of accurate experiments and advanced microscopic theory, (2) these sharpened tools can be applied generally, *e.g.*, to interfaces, where experimental data might be scarce, (3) such applications can easily be chosen from a technological perspective, and (4) even technological applications provide a valuable feedback of fundamental theoretical issues.

In Sec. II the theoretical approach at large is sketched. Section III gives some examples of theoretical methods. In Sec. IV a handful of surface studies are presented. The bridge to, *e.g.*, interfaces is described by a few examples in Sec. V. Section VI illustrates how applications can feed back information and impulses to fundamental theory and exemplify how the fundamental basis can be broadened. Finally, Sec. VII gives a summary and an outlook.

II. APPROACH AT LARGE

The name and overall approach of our Materials- and Surface-Theory group has of course a historical origin. We are fortunate to be scientifically nurtured in the fruitful environment of two excellent experimental surface-physics groups and then stimulated by a national science-council initiative to enter computational materials theory more than a decade ago. However, unlike many computational-materials theorists today that spread their research into surfaces, we have the privilege of starting from the surface platform. Indeed, there is a uniqueness of surface science, with its well-characterized surfaces in an ultra-high-vacuum environment that provide meeting places for numerous accurate experimental techniques and advanced theory. This allows detailed comparisons on the quantum level between experimental data and theoretical results. Such an intellectual driving force develops our theoretical tools and understanding and places us in a good position for broadened applications in, *e.g.*, the world of materials.

A. The surface platform

The materials world, in particular, and science, in general, encompass many important interfaces. Unfortunately, there is typically a shortage of adequate experimental tools to study interfaces. The richness of the class of interfaces can be illustrated by the simple symbol "A — B", where A and B can each belong to any class of material, *e.g.*, metals, insulators, semiconductors, ceramics, polymers, and biomaterials, and can also be in various

structural forms. Other groups of materials phenomena ripe for applications are defects, like vacancies, dislocations, and grain boundaries. Below some studies of interfaces and defects with primarily metals and ceramics are given as examples.

For static properties density-functional theory is a key bridge between surfaces and other interfaces, and this is what is primarily illustrated here. Similarly, other theoretical tools can be sharpened on the surface. This is indicated by two dynamical examples, the theory of single-molecule vibrational spectroscopy and microscopy in inelastic scanning-tunneling spectroscopy and the effect of anisotropic dissipation on the selective bond breaking in surface photochemistry.

The robustness of the surface platform originates from the wealth of experimental probes of surfaces, in addition to the great ability of experimentalists to prepare well-characterized surfaces. There is a tradition to name the experiments by acronyms, and the list of such acronyms is many hundred items long. Low-energy-electron diffraction (LEED), medium-energy ion scattering (MEIS), and scanning-tunneling microscopy (STM) give just the beginning of the list of structural tools. Similarly ultra-violet photoemission (UPS), Auger-electron spectroscopy (AES), and ion-neutralization spectroscopy (INS) for electron structure, and high-resolution electron-energy-loss spectroscopy (HR-EELS), infrared spectroscopy (IRS), and inelastic-neutron scattering (INS) for vibrational spectra. Etc. Also at this symposium several new beautiful experimental techniques have been announced. The tendency is that the experimental information gets more detailed as the acronyms get longer.

The multitude of surface-sensitive probes stems from the facts that surfaces in ultra-high vacuum are available for many test particles and that many physical effects limit many phenomena to the surface region, like electron mean-free paths, cross sections, atom-sized overlaps, surface reflection, and grazing incidence. Over several decades these probes have been developed in an interplay with theory. This results in detailed and well-resolved experimental data, which challenge the development of advanced theory, where a detailed comparison on the quantum level between experimental and theoretical results is possible for a steadily growing number of surfaces and surface phenomena.

B. Challenges of the materials platform

Materials provide many challenges for theory. So far the emphasis has been on static properties, *i.e.* bonding, structure, and energetics, and it will continue to be so, due to the multitude of materials and phenomena. A reminder about the fundamental basis here, density-functional theory, is given below. However, there are a lot of other materials properties, for instance dynamical ones. Each should have a proper description, and the prospect of getting such descriptions is very good, and in some cases already achieved. To be specific we exemplify below with a possible route map for a nonequilibrium description of materials with vital heterostructural properties. In addition, we will give examples of descriptions of phenomena on both the fs and ns scales.

III. DENSITY-FUNCTIONAL THEORY

A. Static phenomena

For static ground-state properties the density-functional theory (DFT)[1–3] provides a general framework for computational methods. The DFT expresses the ground-state energy of an interacting system in an external potential $v(\mathbf{r})$ as a functional $E[n]$ of the particle density $n(\mathbf{r})$, and this energy has its minimum at the true ground-state density[1]. The Kohn-Sham form of the functional makes the scheme a tractable one, as it leads to equations of one-electron type, and accounts for the intricate interactions among the electrons with an exchange-correlation (XC) functional $E_{xc}[n]$.[2] This XC-energy functional can be expressed exactly as an integral over a coupling constant[4–6,3] in the so-called adiabatic-connection formula (ACF).

This equation shows a truly non-local XC interaction and is a starting point for approximate treatments, local (local-density approximation; LDA),[2] semilocal[7] (*e.g.*, the generalized-gradient approximation; GGA) and non-local ones. Today normally the exchange-correlation energy is treated in the generalized-gradient approximation (GGA),

typically the Perdew Wang 91[8] version of GGA (GGA-PW91).[9]

When applying DFT, it is advisable to work with several different methods in the self-consistent total-energy calculations. So far, our calculations are usually performed with the plane-wave pseudopotential method,[9–11] implemented in the `dacapo` code.[12] All the involved elements are described by Vanderbilt ultrasoft pseudopotentials[13] that substantially decrease the necessary number of plane waves in the basis set. The plane-wave cutoff is taken to be some high value that provides a total-energy convergence within typically 0.01 eV/atom. The Brillouin zone is sampled according to the Monkhorst-Pack special-point method.[14] To improve the k-point convergence, the Fermi discontinuity is smoothed, using the Gillan scheme[15] with the effective electronic temperature 0.15 eV.

Also other implementations of DFT are used in our group, for instance, the *ab initio* full-potential linear-muffin-tin-orbital method, which has proven to be one of most accurate techniques for, *e.g.*, studies of phase transitions,[16–18] and a highly parallellized augmented-plane-wave method.[19]

B. Dynamic phenomena

Dynamic properties of materials require a theory base beyond the traditional DFT. However, as a starting point DFT is often very useful. Below we give some examples of such approaches. For vibrationally inelastic tunneling in the STM of an adparticle on a metal surface a DFT-based approach with a many-body generalization of the standard tunneling theory has been developed.[20] For fs-phenomena a dissipative quantum-mechanical method using parallel computers has been applied.[21] For dynamical phenomena over much longer time scales molecular-dynamics and kinetic-Monte Carlo simulations will be mentioned. For dynamics involving the interacting transport through molecular heterostructures we have recently completed a conserving nonequilibrium description of a nanotube heterostructure transistor and have thus documented how conservation laws ensure device robustness.[22]

IV. SURFACE PHENOMENA

Since long, the sharpening of theoretical tools on surfaces, *i.e.* the interplay between the multitude of experiments and advanced microscopic theory has provided models, concepts, results, and ideas.[23] During the past decade a new important addition has been made - the calculation of accurate numbers to compare with accurate experimental numbers. This approach rests on three pillars - (i) computers that get twice as fast every 18th month (Moore's law), (ii) algorithms that successively get more efficient, and (iii) development of the fundamental theory. One of the key themes of this paper is that surface physics is an important driving force for the improvement of the fundamental theory. In particular, this will be illustrated for DFT and its consequences for structure and bonding properties. However, also some examples from dynamics will be shown.

A. Atomic-scale manipulation

Manipulation of individual atoms and molecules on surfaces using STM provides a unique method for producing intentionally ordered atomic-scale structures. There is an ongoing worldwide effort to explore, both experimentally and theoretically, key processes and new methods for controlling manipulations with the STM, in order to provide us with reliable and well-understood manipulation methods at the atomic scale and ultimately to develop an atomic-scale materials engineering.

Results on single-molecule chemistry[24] and single-molecule vibrational spectroscopy and microscopy with STM illustrate the theoretical approach here. First the static properties, like potential-energy surfaces (PES) and local electronic densities of states (LDOS), are calculated in DFT. On this basis results on the dynamical effects of energy transfer are either modelled or explicitly calculated. Two typical cases are referred to, a simple model calculation with realistic parameters and a fully dynamical calculation of the matrix elements involved etc. Successful comparisons with experimental data give promise for such accounts

of dynamical behaviors in more general cases.

The single-molecule chemistry by tunneling electrons has been performed with STM on an oxygen molecule adsorbed on a Pt(111) surface. In addition to the usual structural and electronic information, events of dissociated O_2 molecules are observed as functions of the tunneling current at different sample biases in the temperature range of 40 to 150 K. After dissociation, the two oxygen atoms are found to be one to three lattice constants apart. To explain the characteristic dissociation-rate dependence on the current, we use a dissociation model along the lines of our earlier atomic-switch model.[25] This is a very explicit demonstration of electronic dissipation from adsorbate degrees of freedom to a metal substrate. The rates are thus explained in terms of dissociation induced by intramolecular vibrational excitations via resonant inelastic electron tunneling.

The model has very recently also been successfully applied in an STM study, where all steps of a chemical reaction are induced with the STM tip, described as a step towards single-molecule engineering.[26] All reaction steps have here been successfully induced on individual molecules with an STM in a controlled step-by-step manner, utilizing a variety of manipulation techniques. The reaction steps involve the separation of iodine from iodobenzene by using tunneling electrons, bringing together two resultant phenyls mechanically by lateral manipulation and, finally, their chemical association to form a biphenyl molecule, mediated by excitation with tunneling electrons.

An important breakthrough in vibrational spectroscopy at surfaces has been demonstrated by applying electron tunneling spectroscopy of single molecules on surfaces by an STM.[27–29] Our recent theory of this single-molecule vibrational spectroscopy and microscopy[20] gives vibrational-intensity contours which look very much like the experimental ones. Vibrationally-inelastic tunneling in the STM of acetylene on copper is studied in an approach based on density-functional theory and a many-body generalization of the Tersoff-Hamann[30] theory. It is explained why only the carbon-hydrogen stretch modes are observed in terms of inelastic and elastic contributions to the tunneling conductance. The inelastic tunneling is found to be efficient and highly localized in space without any res-

onant interaction and to be governed by a vibration-induced change in tunneling amplitude. The calculated topographical images of the local density-of-states (LDOS) and of the vibrationally-inelastic tunneling of acetylene on Cu(100) show agreements with measured images in several respects: Local structure and LDOS of C_2H_2; The relative change in tunneling conductance, induced by the C-D stretch mode of C_2HD, mapped out in real space, is highly localized to the C-D bond; The maximum value and the isotope effect of the change in the conductance; For all the modes, except the C-H and C-D stretch modes, the elastic and inelastic contributions tend to cancel.

The vibrational spectroscopy of a single molecule on a surface with STM[27–29]] and its successful comparison with theory[20] illustrate how impressively close present theory and experiment can come to each other today.

B. Long- and intermediate-range adsorbate interactions

STM also allows detailed studies of interactions between adatoms. Atoms and molecules adsorbed on metals affect each other indirectly even over considerable distances. Recent dialogues between theory and experiments have increased our understanding of such interactions in the intermediate and long ranges.

The substrate-mediated long-range oscillatory interaction between adsorbed Cu atoms on Cu(111) has recently been measured and compared to theoretical calculations.[31] A quantitative study of the long-range interaction between single copper adatoms on Cu(111) mediated by the electrons in the two-dimensional surface-state band is compared to the interaction potential determined by evaluating the distance distribution of two adatoms from a series of STM images taken at temperatures of $9 - 21$ K. The long-range interaction is oscillatory with a period of half the Fermi wavelength and decays for larger distances d as $1/d^2$. Five potential minima have been identified for separations of up to 70 Å.

Atoms dropped on the surface can thus interact with one another over long distances. The STM data show that this electron-mediated force is oscillatory in space - alternately

attractive and repulsive, as one atom "rides" the electron waves produced by the other. The interaction leads to rings of attraction and repulsion surrounding each atom, so the results may improve our understanding of the formation of atomic-scale structures on surfaces. Such indirect long-range, oscillatory interactions between adatoms have been suggested long ago.[32,33] Until now, however, no one has directly measured them, due to their weakness; the corresponding energies are less than 1 meV. The new experimental data for the scattered electron waves are in rough agreement with the theoretical predictions.[31]

C. Growth

Indeed, atoms and molecules adsorbed on metals affect each other indirectly over a considerable range of distances. At intermediate distances it is necessary to consider both the substrate-mediated elastic interaction[32] and the nonasymptotic part of the indirect electronic interaction. These types of interactions have recently been investigated experimentally by STM measurements[34] and theoretically by density-functional calculations.[35]

While DFT calculations of interactions of nearby adatoms today are more or less standard, such calculations in the long and intermediate ranges still require a real tour de force of computation, due to the size of the problem. Systematic density-functional calculations have recently in this way contributed to the establishment of the nature and strength of such interactions and the explanation for what important materials properties of the adsorbate systems are critically affected.[35]

Via these calculations the nature and strength of such interactions are established and explained in terms of adsorbate systems, where they critically affect important materials properties. The latter is verified in kinetic Monte-Carlo simulations of epitaxial growth, which show radical differences in aggregation at low temperatures for the cases with and without adsorbate interactions (Fig. 1) and help rationalize a number of recent experimental reports on anomalously low diffusion prefactors. Our suspicions about the anomalous prefactors are now experimentally confirmed.[36]

This study is a part in a series of metallic-growth investigations. The first-principles approach started with calculations of low-symmetry diffusion barriers in homoepitaxial growth of Al(111).[37] Actually, the exotic variety of surface morphologies, from fractals to compact islands, offered by epitaxial growth emanate from a handful of elementary atomic diffusion processes. With extensive density-functional calculations on parallel computers barriers for self-diffusion at steps, kinks, and corners on Al(111) are mapped out. An unexpected exchange-diffusion mechanism at kinks is revealed, and a large anisotropy at corners is shown. Other results are used to predict various growth modes and their active temperature intervals. Several predictions have recently been confirmed by STM experiments.[39]

The dynamics of Al dimers on Al(111) at equilibrium and under compression has also been studied with first-principles DFT calculations.[38] A smooth potential-energy surface provides an attraction between the dimer atoms and leads to a substantial temperature window, in which dissociation is frozen and exotic dimer dynamics is observed. Surface relaxations play a prominent role in the uncovering of an unexpected ground state and a new diffusion path. A way of affecting growth by compression is illustrated.

While our early attempts have used a simplified Arrhenius-law argument to relate the energetics of elementary diffusion processes to growth morphology,[37] such questions are now addressed by kinetic Monte Carlo (KMC) simulations.[40] The microscopic origin of compact triangular islands on close-packed surfaces has been identified using KMC simulations based on energy barriers from DFT calculations.[41] In contrast to earlier accounts, corner diffusion anisotropy is found to control the shape of compact islands at intermediate temperatures. The correlation between the orientation of dendrites grown at low temperatures and triangular islands grown at higher temperatures is rationalized, and the fact that in some systems dendrites grow fat before turning compact is explained.

Open surfaces behave differently from dense ones. Atom-by-atom and concerted hopping of ad-dimers on open (100) surfaces of fcc metals have also been studied by means of DFT calculations.[42]. The adatom interaction is relatively short ranged, and beyond next-nearest neighbors ad-dimers are effectively dissociated. Diffusion takes place by a simple shearing

process, favored because it maximizes adatom coordination at the transition state. This holds for Al, Au, and Rh, and is likely to be a general result, because geometrical arguments dominate over details of the electronic structure.

D. Dissipative quantum dynamics

Growth provides examples of dynamical phenomena in materials that extend over long times. There are also phenomena occurring on the fs scale characteristic of electronic interactions. Dynamics of a local mode coupled to a heat bath is of broad interest in physics and chemistry. Such a coupling often leads to energy transfer and dissipation, which helps to keep the system in equilibrium with the bath. The effect of dissipation in a short-time process has been studied for the two-dimensional dissipative quantum dynamics (DQD) of O_2/Pt(111), where the system is far away from equilibrium with the bath.[21] This is an ideal and well-characterized model system.

Photochemistry of this system has been studied by various experimental techniques, including ns- and fs-laser pulses.[43–46] Well-documented data thus provide a unique testing ground for short-time dynamics. The DQD has been solved by a stochastic wavepacket approach and parallel-computing techniques. The anisotropic dissipation on the potential energy surface (PES) is found to create nonequilibrium and anisotropic energy storage on short time between different reaction channels. The latter determines decisively the short-time reaction dynamics and in particular the branching ratio between desorption and dissociation, in quantitative agreement with recent experimental findings.[21]

In particular, the branching ratio (BR) between desorption and dissociation can be controlled selectively by varying the duration of the laser pulse. With ns pulses, the BR is around 0.5 - 1.0. With fs pulses it is more than one order of magnitude larger (BR = 5 - 30).[44,45] Similar observations apply to O_2 on Pd[47] and on stepped Pt surfaces.[46] These experiments demonstrate the possibility to selectively break a surface bond at will. For long, the mechanism and the dynamics of the achieved selectivity have remained puzzling issues in surface

photochemistry and cannot be explained in terms of the dynamics without dissipation.[48] Now the DQD of the O_2/Pt(111) has been solved on its PES in two dimensions, including the molecule-surface and the intra-molecular coordinates. Dissipation due to coupling to the metal electrons has been included explicitly, using the recently-developed Lindblad approach[49] for DQD.[50,51] The DQD clearly shows that anisotropic dissipation between the two coordinates creates an inhomogeneous density profile of molecules on a subpicosecond timescale, determining the short-time dynamics of vibrational relaxation and, in particular, the selective bond-breaking, before the molecules re-establish equilibrium with the surface. These results clearly demonstrate a key role of dissipation in surface photochemistry and have general implications on other nonequilibrium phenomena in condensed phases.

E. Dissociation of O_2 on Al(111)

The oxidation of metal surfaces is a phenomenon of outstanding practical importance. In particular, the oxidation of aluminum surfaces has been a long-standing subject of study, raising several still controversial issues.

An extensive first-principles DFT study of large pieces of the adiabatic potential-energy hypersurface has been performed for O_2 adsorption on the Al(111) surface (Fig. 2).[52,53] These calculations show that an O_2 molecule approaching the surface adiabatically has an entrance-channel barrier *only* in one out of eight considered entrance channels for the parallel case, *i.e.* when the molecular axis is kept parallel to the surface, while the non-parallel case has a molecularly chemisorbed state, an "O_2^{2-}" precursor to an activated dissociation. The predicted metastable molecular state is stabilized by a Hund's-rule spin correlation effect on the very inequivalent oxygen atoms of the non-parallel O_2 molecule in the strong Al-surface field on the electrons. It provides a source for abstraction, *i.e.* dissociative decay by emission of one oxygen atom, and it also gives a basis for single and close-paired O adsorption.

One consequence of the calculated PES is that the dissociation of an oxygen molecule can occur via abstraction, *i.e.* emission of one oxygen atom[54,55] and chemisorption of the

other one. The O_2 molecule should be energetically favored to be oriented with its axis more or less normal to the surface. After dissociation, one of the O atoms should be adsorbed on the surface near the point of impact, while the other atom should be repelled and fly away from the surface or transferred along it over a large distance.[56] A recent laser and STM study of the O_2/Al(111) system[57] provides compelling evidence for the abstraction mechanism and for isolated and dimer oxygen on the surface. At a translational energy of 0.5 eV the dissociative chemisorption of oxygen is documented to give both abstraction of neutral O atoms, uncorrelated atomically adsorbed O atoms, and correlated ones in neighboring fcc sites as end products. The existence of correlated atomically adsorbed O atoms in neighboring fcc sites is also confirmed by a recent STM study.[58] The calculated potential-energy surface also shows that oxygen adsorption on this surface is an intricate and complex process. There are expected features, *e.g.*, charge transfer, and novel ones, such as a pronounced orientational dependence.

Similar calculations have been performed for NO, N_2, and CO on Al(111), revealing interesting trends.[59]

V. TOWARDS INTERFACE PHYSICS

In summary, there is a wealth of experimental probes for surfaces. In addition, the experimentalists have a great ability to prepare well-characterized surfaces. In parallel, there is a strong development in advanced theory. Taken together, there is a basis for detailed comparisons on the quantum level between experimental and theoretical results. This in turn provides a basis for further development of the theory and of our understanding. In this way surfaces provide grindstones to sharpen our theoretical tools.

The prime example concerns static properties and DFT. A worldwide effort here pushes for successive improvements in the basic theory, *i.e.* in the exchange-correlation functional,[60] and in the methods to solve the DFT equations. Due to the large inhomogeneity of the electron-density distribution at the surface, the surface platform sets extra requirements on

both features. General methods that apply accurately at surfaces are likely to be broadly applicable. We will exemplify this by some recent bulk and interface applications of our group.

A. Theoretical determination of bulk structure - κ-alumina

Static materials properties to address directly with the DFT are stability, bonding, and structure.

An industrial champion on the board of our materials consortium has drawn our attention to the κ-phase of Al_2O_3, relevant for wear resistant cutting-tool coatings (WC/Co/Ti(C,N)/κ-Al_2O_3/TiN). Due to its structural variety, alumina has many applications: for instance, α-Al_2O_3 in electronics, γ-Al_2O_3 in catalysis, and κ-Al_2O_3 as chemically-inactive wear-resistant coating on cemented-carbide cutting tools. Although metastable, κ-Al_2O_3 appears to be quite stable, maintaining its structural identity up to temperatures of about 1200 K, where it transforms to α-Al_2O_3. At the start of our study this structure was unknown, and yet it should be valuable to know it for the chemical-vapor-deposition (CVD) process used in the manufacturing of the tools.

There are questions about the mechanism behind the CVD growth process, about the sometimes favored growth of α-Al_2O_3 sometimes before that of κ-Al_2O_3, about the occasional coexistence of the two phases on the same substrate, and about the phase transition from κ to α. To answer these, the first step is to determine the atomic structure.

From a theoretical perspective, κ-Al_2O_3 is a system that is too complex to be efficiently described in terms of simple model potentials for the interactions between the atoms.[61] At the same time it is a challenge for first-principles methods because of its relatively large unit cell, composed of 40 atoms, and the difficulties involved in the description of the tightly-bound valence electrons of the oxygen atoms.

In a massive first-principles DFT study of bulk κ-Al_2O_3 the atomic and electronic structures have been determined with DFT, plane waves and pseudopotentials.[64] Out of 60 "ideal"

independent structural candidates for κ-Al_2O_3 - using what was known about symmetry etc. - relaxation of the atomic positions according to the fundamental laws of DFT has been allowed, and finally a single stable structure has been singled out (Fig. 3). The calculated atomic structure has been proved to be correct by X-ray diffraction (XRD) experiments performed during the process.[62–65] The bonding is highly ionic, and the insulating properties are ensured by a large gap, almost as high as that of α-Al_2O_3.

This and similar works show that it today is possible to theoretically determine the atomic structure of complex technologically important materials. This fortunate situation has been achieved thanks to the combination of improving theoretical methods, especially those based on DFT, more efficient computational algorithms, and rapidly growing computer power, including parallelization.

The now theoretically and experimentally determined κ-Al_2O_3 bulk structure[62–65] is a valid starting point for studying surfaces and their structure and stability. In particular, general results to elucidate the role of tetrahedrally-coordinated Al (Al^T) in the alumina-surface characteristics is highly desirable. Structurally, while α-Al_2O_3 has Al in only octahedral coordination (Al^O), metastable aluminas have a mixture of Al^O and Al^T.

First-principles DFT calculations with the `dacapo` code have also been made to study the (001) and $(00\overline{1})$ surfaces of κ-Al_2O_3, with comparisons to the stable-phase α-Al_2O_3(0001) surface.[66] Due to the low symmetry of the κ-Al_2O_3 crystal, κ-Al_2O_3(001) and $(00\overline{1})$, created by cutting the single crystal perpendicularly to the c-axis, are inequivalent. Also, for each facet there are several possible termination types.

The most stable (001) surface is non-polar and terminated with a semifull Al layer. Octahedral sites are preferred over tetrahedral ones at the surface. This is understood in terms of a general Pauling-rules type of argument and should be applicable to other metastable aluminas as well. Due to the strong electrostatic forces and open structure, the surface Al undergo a giant relaxation, yielding an O-terminated surface. The ionic character is conserved after relaxation.[66]

The corresponding $(00\overline{1})$ surface undergoes a smaller, although still large, relaxation, of

a magnitude similar to that of α-Al_2O_3(0001). However, a possible polarity of this surface is detected after relaxation, accompanied by the presence of a metallic surface state (Fig. 4). These polarity effects should be important for the relative stability of the κ-Al_2O_3 growth in the [001] *vs.* the $[00\overline{1}]$ directions.[66]

B. Pressure-induced phase transitions - Ga and In

First-principles DFT calculations are ideal tools to study materials under high pressure P, provided appropriate extensions are made. In the bulk, phase transitions can be induced, as illustrated in the literature for many classes of materials. One interesting group in the periodic table is group IIIa. Here Al remains in the fcc structure up to P equal to 220 GPa. Ga and In crystallize in unusual open ground-state structures. Ga is orthorombic at ambient pressure, converts to bct at about 14 GPa, to have a phase transition to fcc at 82 or 120 GPa. For In, which has the bct structure, no phase transition has been observed yet.

First-principles DFT calculations with a FP-LMTO method provide in simple terms an explanation for this difference in behavior. In addition, they predict a so far undiscovered transition of In to a close-packed structure at extreme pressures and show the structure-determining mechanism to originate from the degree of $s-p$ mixing of the valence orbitals, so the phase transitions are driven by an optimization of $s-p$ hybridization. In general, the group-III elements are shown to strongly disobey the standard corresponding-state rule.[67]

C. Dislocations in metals

The description of a dislocation starts with the ideal crystal and its perfect stacking. When a stacking fault is created here, the extra plane gives the dislocation. The microscopic account of an edge dislocation focuses on the general stacking-fault energy γ_{GSF}, which relates to the excess energy caused by the sliding in a direction characteristic for the dislocation.

By first-principles DFT one can calculate this energy. Then one practical limitation is set by the size of the supercell - the unit containing the "active" atoms. Today it is possible to work with supercells of an interesting size. Another challenge is the smallness of the energies involved. Stacking-fault-energy values for semiconductors are relatively high and can to some extent be accounted for in simple but physically sound models.[68] In metals the values are small and the procedure more demanding.

The stacking-fault energy has been calculated for some metals[69]. With increasing displacement it typically first grows linearly and then smoothly saturates, to finally get slightly reduced. This stacking-fault energy can then be used in the Peierls-Nabarro model[70] and be related to macroscopic quantities.

D. Interface energy for VN/Fe

Our initial interface calculation has concerned the interface between vanadium nitride and iron.[71] The motivation is metallurgical. In steels non-shearable precipitates are obtained with carbide and nitride formers, such as Ti, V, Cr, and Nb. Precipitates with the NaCl structure is one important class and are often found as small thin discs, with a radius of 50 - 100 Å. The 'flat' part of the interface is semi-coherent, *i.e.* has a small misfit-dislocation density. The 'side', on the other hand, has a large lattice mismatch and is incoherent with the Fe matrix. These small precipitates form within grains, contrary to other carbides and nitrides, which preferably form on grain boundaries. Knowledge about nucleation and growth of such precipitates is necessary in order to predict long-time structural changes in steel. In particular, modeling on a thermodynamical basis provide means to improve high-temperature creep resistance.

The atomic and electronic structures in a model system of the semi-coherent interface between bcc-Fe and nacl-VN have been calculated.[71] The total energy is calculated with pseudopotentials, planewaves, and GGA in `dacapo`. The Fe/VN interface energy is found to be very small. This contributes to the understanding of why alloying with V and N blocks

dislocation motion and yet keeps up the strength of the steel, as the incentive for the VN grains to grow should be very small. The calculation points out features of the electron structure that make the formation of very small VN precipitates in Fe favorable.[71]

E. Wetting in sintering - TiC/Co

Many great advances of modern materials engineering come from the area of composite materials. The outstanding performance characteristics (strength, etc.) of those materials have already found a wide range of practical applications, from cutting tools and sporting goods to space ships. There are many different kinds of composites, but, at the most basic level, the idea of all composites is to combine two or more distinct materials to produce a heterogeneous mixture that performs significantly better than any of its components by itself. In many cases it is a great challenge to understand why this can work, and what are the microscopic mechanisms behind such a behavior. Figure 5 provides one interesting example where this type of behavior can be easily seen at the level of atoms and electrons.[72]

The above figure is a result of quantum mechanical simulations of an interface between Co-metal and TiC-ceramic, a representative case of interfaces in cermet hardmetals (metal-ceramic composites), which are used as advanced-tool materials. The figure shows the spatial distribution of the electron density (a constant density surface at the level of 0.5 electrons per cubic Å) in the interface region. It illustrates the difference between the types of chemical bonding in the ceramic (on the left), the metal (on the right), and at the interface (in the middle). It is interesting to note that the chemical bonds at this heterointerface are drastically stronger than what can be reached in homogeneous compounds of the elements involved. So, in short, we get strength from dissimilarity.

In more detail, by means of first-principles DFT computational experiments, performed with the `dacapo` code, the microscopic mechanism of metal-carbide adhesion is revealed.[72,73] The DFT results for the Co/TiC(001) interface show the interface bonding to be dominated by Co-C bonds. The effective number of bonds is controlled by an interplay between lattice

mismatch and relaxation effects. The particular strength of the Co-C bond is explained in terms of interface-induced features of the electron states, in particular a novel metal-modified covalent bond. The calculated adhesion strength agrees with results of wetting experiments.[72]

F. Vacancy formation

Aluminum has been named the "hydrogen atom" of computational materials science. In a recent letter[74] vacancies in metals are addressed with first-principles DFT calculations, using the `dacapo` code. The calculated value of the mono-vacancy formation energy is compared with the experimental one. An apparent inability of density functional theory (DFT), within the LDA and GGA approximations, to, *e.g.*, describe vacancies in Al accurately and consistently is implied and a resolution is suggested. The shortcoming should be due to electron-correlation effects near electronic edges. A correction method is shown.

This calculation indicates that even internal surfaces can provide testing cases for fundamental theory. In this case it is implied that local and semi-local accounts of exchange and correlation effects should be insufficient in such a case with large inhomogeneities (Fig. 6) and call for a truly non-local exchange-correlation functional.

G. Strength of materials and length scales

In the description of materials strength it is natural to work on three length scales, the microscopic, the mesoscopic, and the macroscopic ones. The ultimate theory will integrate these scales. Materials properties depend, indeed, on the atoms that constitute the material. The electron-structure theory primarily gives results on the microscopic scale, and here atomic-scale accounts of, *e.g.*, interfaces, dislocations, and vacancies are typical illustrations. Below we will also give an example of how to bridge the scales, taken from the world of liquid crystals. However, the illustration can just as well be, *e.g.*, the Peierls-Nabarro model for the area of dislocations.[70]

H. Length scales in materials - nematic liquid crystal

As an example of a realistic way of connecting macro-, meso-, and microscales a recent study of a nematic liquid-crystal confined between two horizontal plates can be mentioned.[75] Here, a general analytical solution for the field describing the local liquid-crystal molecular orientation is provided in the presence of an applied electric or magnetic field. The effect on the bulk orientation by imposing various molecular directions (anchoring angles) at the confining plates is derived and analyzed, and predictions for the resulting, experimentally observable, optical response are presented.

In this case the microscopic input is the local molecular orientation at the surfaces of the plates. Such a quantity can, in principle, be calculated by first-principles DFT calculations. A research program in this direction is in progress. For soft matter, as in liquid crystals, van der Waals forces are judged to be important. In a DFT approach thus the exchange-correlation density functional should have a non-local density dependence relevant for the van der Waals interactions.

The method of bridging the length scales of materials by an intermediate mesoscopic analytical model is expected to have bearings on other classes of materials, as well. In the following there is an attempt to briefly describe our attempts towards this goal.

VI. FEEDBACK AND RESPONSE

For some theorists it might seem a little frightening to study practical, industry-related materials problems. As a matter of fact, it is the opposite. We have found it very rewarding, not only in the broad sense of maybe making something useful for Society but also in the narrow senses of broadening your materials horizon and giving feedback to fundamental theory. This type of feedback is amply demonstrated in the literature, and some examples are given above.

Here only one example of how practical problems put demands on fundamental theory

will be touched upon. Several calls for an improved DFT have been made above, most explicitly for a non-local density-functional:

The above account of the O_2 molecule at the Al(111) surface has several implications that are confirmed by experiment. However, there is a key experimental result that is not accounted for by the calculated adiabatic potential-energy surfaces: The initial sticking probability for low kinetic energy of the incoming molecules has a very low value. Maybe a diabatic description could do so. This might require some temporary precursor state for O_2 before any charge transfer has occurred. The corresponding potential-energy surface should be one for a neutral O_2 molecule, *i.e.* an entity that is attracted to the surface only by van der Waals forces. However, the molecule-surface separation is too short for the common asymptotic forms of the van der Waals interaction to apply. Consequently, there is a need for a non-local density functional that accounts for the saturated van der Waals interaction at intermediate and short distances.

As described above, the calculation of the vacancy-formation energy of Al calls for a non-local exchange-correlation energy functional.

For soft matter the calls for adequate accounts of van der Waals interactions are more general. The liquid-crystal case above indicates this, but there are numerous other applications, like such that involve water, polymers, fullerenes, and biomolecules.

In short, a non-local exchange-correlation density functional that accounts for van der Waals effects (vdW-DF) is strongly wanted.

A. Density functional for van der Waals forces in asymptotic limit

The ubiquitous van der Waals interaction needs an efficient and accurate description in many contexts, such as interacting noble-gas atoms, van der Waals complexes, physisorption, interacting macroscopic neutral bodies, liquid-crystal interactions, solute-solvent interactions, and soft condensed matter. For dense matter DFT,[1] with its LDA[2,5] and GGA,[7,76,9,77] is a clear success. Ground-state and thermodynamic properties of increasingly more com-

plex systems are now being calculated with a practically very useful accuracy. As the world around contains far more objects than just hard solids, a generalization of these methods to also account for the van der Waals forces is in great demand. These forces are an inherent property of the exact DFT,[78] and it is thus a question of providing an approximate van der Waals density functional that is generally applicable, efficient, and accurate, and that per definition is a functional of the density only. Early proposals for such functionals have shown them to give useful results in significant applications.[79–82] Their asymmetry in the treatment of "small" and "large" objects, respectively, has been remedied in a recent "unified" treatment.[83]

Starting from the exact ACF expression for the exchange-correlation energy $E_{\rm xc}$ as an integral over the coupling constant,[5,4] two approximations allow the setting-up of an appropriate density functional for two separated objects. First a local dielectric function is introduced that depends on the local electron density. Second, we limit the volumes of the interacting objects by using a cutoff,[84] outside which the response to an electric field is defined to be zero. These approximations are common for all three studied model systems – interacting atoms or molecules,[79,85] an atom or molecule interacting with a planar surface,[80,86] and finally two interacting surfaces.[87]

Unification means that local electrodynamics, *i.e.* a local relationship between the polarization $\mathbf{P}$ and the total electric field $\mathbf{E}$ is applied. In a framework for long-range DFT thus a unified full-field treatment of the asymptotic van der Waals interaction for atoms, molecules, surfaces, and other objects is available. The inputs that are needed are the electron densities of the interacting fragments and the static polarizability or the static image plane, which can be easily evaluated in a ground-state density-functional calculation for each fragment. So, in this approach there is no analytical functional of the density that takes care of it all. Rather there is a simple such functional that has to be supplemented with an extra calculation of the Kohn-Sham equations, now in the presence of a weak electric field. Thanks to general features of polarization properties, already the static polarizability etc. contains key information. Results for separated atoms, molecules, and for atoms/molecules

outside surfaces are in agreement with those of other, more elaborate, calculations.

This general density functional for asymptotic van der Waals forces has been used to calculate van der Waals (vdW) coefficients and reference-plane positions for realistic low-indexed Al surfaces, with results for a number of atoms and molecules outside the surfaces, as well as for the interaction between the surfaces themselves.[88] The densities and static image-plane positions that are needed as input to the vdW functional are calculated self-consistently within DFT using the GGA, pseudopotentials, and plane waves. This study shows that the vdW-DF is applicable to realistic surfaces. The need for physically correct surface models, especially for open surfaces, is also illustrated. Finally the parameters for the anisotropic interaction of O_2 with Al is calculated.[88]

B. Tractable van der Waals density functionals for two close flat surfaces and slabs

In order to allow DFT to describe sparse matter the DFT needs improvements that include non-local effects, such as vdW forces.[78,79,81,80,82,87,89,83] The ultimate challenge is to construct an approximate vdW-DF that is generally applicable, efficient, and accurate, also at short distances and at non-zero overlap. Knowing the complex origin of the vdW interaction, it might seem deterrent to even try to get it accounted for by just a functional of the density. The challenge is met in a few cases, like an accurate calculation for the interaction of two He atoms,[82] and a RPA calculation for two self-consistent jellium slabs.[89]

As another step forward towards a practical functional, an explicit form for the vdW-DF that applies to flat surfaces has been proposed.[90] It has been tested successfully against the results from the mentioned microscopic calculation of the vdW interaction between two self-consistent jellium slabs.[89] An application has also been made to two parallel flat semi-infinite metal surfaces (Fig. 7), a case with relevance for many physical situations, including wetting and atomic-force microscopy (AFM). Compared to the vdW-DF approximation proposed by Dobson and Wang,[89] the virtues of our functional are the computational simplifications gained from choosing a particular sub-class of response functions, utilizing a differential for-

mulation and sparse matrices, and recognizing the insensitivity to the details of the density profiles, simplifications which might transfer even to three dimensions. The present systematic approach for the construction of a density functional for van der Waals interactions accounts for saturation effects, *i.e.* it should apply at short distances.

C. Application to graphene and similar systems

At large separations d between the interacting objects the van der Waals potential attains its asymptotic form. This form is a power law, $-1/d^n$, where the exponent n depends on the geometry, with characteristic values for two parallel flat semi-infinite objects ($n = 2$), for sphere outside flat surface ($n = 3$), for two sheets ($n = 4$), for two spheres ($n = 6$), etc. The asymptotic form of course stops to be valid long before the d value is close to the singularity, for real objects typically measured from a van der Waals plane,[91] etc. The true interaction is certainly not singular, and it is an important research to account for the saturation, *i.e.* the correction to the singularity at small and intermediate separations.

The proposed saturated vdW-DF[90] has so far been applied to jellium (see above),[90] and various interactions of graphene, *i.e.* a single sheet of carbon atoms arranged like in a layer of graphite.[92] For graphene the electron density and the induced density have been calculated with DFT in the LDA and GGA, respectively, and then the vdW-DF model parameter q_{perp} is fitted to the calculated static polarizability.[92] The preliminary results of the binding-energy of these two graphene sheets are as follows: The LDA results for the difference in the energy values at separation d and at infinite separation look like a common binding-energy curve. The GGA curve is repulsive, however! Now, as described above, the non-local vdW interaction is fundamentally absent in both LDA and GGA. At the same time graphite and graphene are, indeed, true prototype systems for the vdW interaction. So both the LDA and GGA results are basically wrong (As a historical comment, the fact that LDA happen to give reasonable results for the binding might even be considered to be unfortunate). At the relevant separation values (about 3 - 4 Å) the inhomogeneity length

is simply too unfavorable compared to local screening lengths etc. to allow local and semi-local approximations.[93] Their only role can be as platforms for application of non-local vdW corrections. When our vdW-DF correction is added to the GGA result, the full binding-energy curve is obtained. This preliminary "GGA + vdW" binding-energy calculation gives a binding-energy value of 10.3 meV/Å^2 (13 $\pm$ 3 meV/Å^2) at the equilibrium interplanar distance 3.34 Å (3.35 Å) in the ABAB stacking, where the values within parenthesis are experimental numbers, and 7.15 meV/Å^2 at 3.67 Å in the AAAA stacking.[92]

There is an impressively close relation between the graphene-graphene binding energy and equilibrium distance in experiment and in our "tractable" approximation.[90] The following simple story can be told: (1) LDA gives good binding but for wrong reason; (2) GGA gives repulsion; (3) the GGA plus vdW(tractable) results for graphene look very encouraging; (4) It is even found that GGA plus the traditionally used asymptotic vdW formula gives a sizable error in binding energy and equilibrium separation.[92]

However, at the time of writing, the formal proof for the GGA plus vdW procedure remains to be given. Certainly in Ref. 90 we have effectively added our result to an RPA version of LDA, in order to compare with the exact RPA result. Further, the Langreth-Mehl functional[7] should be added to the RPA version of the LDA. The long-range part of our vdW correction should be mostly contained within the RPA, but the intermediate range part may not be. Another issue to address before the application of our vdW approximation is the fixing parameters of the model vdW-DF. So far, the preliminary graphene results are given primarily as a thought-provoking progress report.

The key point of this section - that practical problems put demands on fundamental theory - is certainly given an explicit illustration in the case of a non-local density-functional.

VII. CONCLUSIONS AND OUTLOOK

This brief review is an attempt to illustrate the scope of this international symposium - to bring together recent advances in experimental and theoretical approaches of surfaces

and interfaces as different symmetry crossings. The illustration is taken from the area of computational materials physics. Many groups around the world are contributing to the presently very rapid progress of this area. Here the emphasis is on experiences from our Materials- and Surface-Theory group. On this basis some theses are formulated:

(1) Surfaces provide platforms to sharpen our theoretical tools, thanks to a multitude of accurate experiments and advanced microscopic theory;

(2) These sharpened tools can be applied generally, *e.g.*, to interfaces, where experimental data might be scarce;

(3) Such applications can easily be chosen from a technological perspective; and

(4) Even technological applications provide valuable feedbacks of fundamental theoretical issues.

For the future, a powerful role of theory, modeling, and simulations (TMS) can be envisaged in materials science, being the motor in materials research, development, and design. This certainly does not downplay the role of experiments, but TMS now is able to shoulder the burden to stimulate, focus, interpolate, and extrapolate. The recent and present strong progress of many TMS groups and networks over the world gives a basis for the ongoing paradigm shift in materials science.

REFERENCES

[1] P. Hohenberg and W. Kohn, Phys. Rev. **136**, B864 (1964).

[2] W. Kohn and L. J. Sham, Phys. Rev. **140**, A1133 (1965).

[3] R. O. Jones and O. Gunnarsson, Rev. Mod. Phys. **61**, 689 (1989).

[4] D. C. Langreth and J. P. Perdew, Solid State Commun. **17**, 1425 (1975).

[5] O. Gunnarsson and B. I. Lundqvist, Phys. Rev. B **13**, 4274 (1976).

[6] D. C. Langreth and J. P. Perdew, Phys. Rev. B **15**, 2884 (1977).

[7] D. C. Langreth and M. J. Mehl, Phys. Rev. Lett. **47**, 446 (1981).

[8] J. P. Perdew, in *Electronic Structure of Solids*, edited by P. Ziesche and H. Eschrig (Akademie Verlag, Berlin, 1991).

[9] J. P. Perdew, J. Chevary, S. H. Vosko, K. Jackson, M. R. Pederson, D. Singh, and C. Fiolhais, Phys. Rev. B **46**, 6671 (1992), 48 4978(E) (1993).

[10] G. Kresse and J. Furthmüller, Phys. Rev. B **54**, 11169 (1996).

[11] G. Kresse and J. Hafner, J. Phys.: Condens. Matter **6**, 8245 (1994).

[12] L. B. Hansen *et al*, dacapo-1.30, CAMP, DTU, Denmark.

[13] D. Vanderbilt, Phys. Rev. B **41**, 7892 (1990).

[14] H. J. Monkhorst and J. D. Pack, Phys. Rev. B **13**, 5188 (1976).

[15] M. J. Gillan, J. Phys.: Condens. Matter **1**, 689 (1989).

[16] M. Wills, unpublished.

[17] J. M. Wills and B. R. Cooper, Phys. Rev. B **36**, 3809 (1987).

[18] S. I. Simak, U. Häubermann, I. A. Abrikosov, O. Eriksson, J. M. Wills, S. Lidin, and B. Johansson, Phys. Rev. Lett. **79**, 1333 (1997).

[19] S. Gao, to be published.

[20] N. Lorente and M. Persson, Phys. Rev. Lett. **85**, 2997 (2000).

[21] S. Gao, J. Strömquist, and B. I. Lundqvist, Phys. Rev. Lett. **86**, Feb 26 (2001).

[22] P. Hyldgaard and B. I. Lundqvist, Solid State Commun. **116**, 569 (2001).

[23] See, *e.g.*, B. I. Lundqvist, Chapter 8 in "Interactions of Atoms and Molecules with Solid Surfaces", Ed. M. Tosi, Plenum Publishing Corporation, (1990), pp. 213 - 254.

[24] B. C. Stipe, M. A. Rezaei, W. Ho, S. Gao, M. Persson, and B. I. Lundqvist, Phys. Rev. Lett. **78**, 4410 (1997).

[25] S. Gao, M. Persson, and B. Lundqvist, Phys. Rev. B **55**, 4825 (1997).

[26] S.-W. Hla, L. Bartels, G. Meyer, and K.-H. Rieder, Phys. Rev. Lett. **85**, 2777 (2000).

[27] B. C. Stipe, M. A. Rezaei, and W. Ho, Science **280**, 1732 (1998).

[28] B. C. Stipe, M. A. Rezaei, and W. Ho, Phys. Rev. Lett. **81**, 1263 (1998).

[29] B. C. Stipe, M. A. Rezaei, and W. Ho, Phys. Rev. Lett. **82**, 1724 (1999).

[30] J. Tersoff and D. R. Hamann, Phys. Rev. Lett. **50**, 1998 (1983), Phys. Rev. B **31**, 805 (1985).

[31] J. Repp, F. Moresco, G. Meyer, K.-H. Rieder, P. Hyldgaard, and M. Persson, Phys. Rev. Lett. **85**, 2981 (2000).

[32] K. H. Lau and W. Kohn, Surf. Sci. **65**, 607 (1977).

[33] K. H. Lau and W. Kohn, Surf. Sci. **75**, 69 (1978).

[34] L. Österlund, M. Ø. Pedersen, I. Stensgaard, E. Lægsgaard, and F. Besenbacher, Phys. Rev. Lett. **84**, 4812 (1999).

[35] A. Bogicevic, S. Ovesson, P. Hyldgaard, H. Brune, B. I. Lundqvist, and D. R. Jennison,

Phys. Rev. Lett. **85**, 1910 (2000).

[36] H. Brune *et al*, to be published.

[37] A. Bogicevic, J. Strömquist, and B. I. Lundqvist, Phys. Rev. Lett. **81**, 637 (1998).

[38] A. Bogicevic, P. Hyldgaard, G. Wahnström, and B. I. Lundqvist, Phys. Rev. Lett. **81**, 172 (1998).

[39] J.V. Barth, H. Brune, B. Fischer, J. Weckesser, K. Kern, Phys. Rev. Lett. **84**, 1732 (2000).

[40] A. Voter, Phys. Rev. B **34**, 6819 (1986).

[41] S. Ovesson, A. Bogicevic, and B. I. Lundqvist, Phys. Rev. Lett. **83**, 2608 (1999).

[42] A. Bogicevic, S. Ovesson, B. I. Lundqvist, and D. R.Jennison, Phys. Rev. B **61**, 2456 (2000).

[43] *Laser Spectroscopy and Photochemistry on Metal Surfaces*, edited by H. L. Dai and W. Ho (Singapore, World Scientific, 1995).

[44] F. J. Kao, D. G. Busch, D. G. da Costa, and W. Ho, Phys. Rev. Lett. **70**, 4098 (1993).

[45] D. G. Busch and W. Ho, Phys. Rev. Lett. **77**, 1338 (1996).

[46] C. E. Tripa and J. T. Yates, preprint.

[47] J. A. Misewich, S. Nakabayashi, P. Weigand, M. Wolf, and T. F. Heinz, Surf. Sci. **363**, 204 (1996).

[48] J. Strömquist and S. Gao, J. Chem. Phys. **106**, 5751 (1997).

[49] G. Lindblad, Commun. Math. Phys. **48**, 119 (1976).

[50] S. Gao, Phys. Rev. Lett. **79**, 3101 (1997).

[51] S. Gao, Phys. Rev. B **60**, 15609 (1999).

[52] Y. Yourdshahyan, Ph. D. thesis, Chalmers Univ. Techn. and Göteborg Univ., Göteborg,

Sweden (1999), ISBN 91-7197-763-5.

[53] Y. Yourdshahyan, B. Razaznejad, and B. I. Lundqvist, Solid State Commun. (2000), in print.

[54] L. Hellberg, J. Strömquist, B. Kasemo, and B. I. Lundqvist, Phys. Rev. Lett. **74**, 4742 (1995).

[55] J. A. Jensen, C. Yan, and A. C. Kummel, Science **267**, 493 (1995).

[56] J. Strömquist, L. Hellberg, B. Kasemo and B. I. Lundqvist, Surf. Sci. **352**, 435 (1996).

[57] M. Binetti, O. Weisse, E. Hasselbrink, A. J. Komrowski, and A. C. Kummel, Faraday Discuss. **117**, 313 (2000)

[58] M. Schmid, private communication.

[59] B. Razaznejad and B.I. Lundqvist, to be published.

[60] See, e.g., B. Hammer, L. B. Hansen, and J. K. Nørskov, Phys. Rev. B **59**, 7413 (1999).

[61] M. Wilson, M. Exner, Y. Huang, and M. W. Finnis, Phys. Rev. B **54**, 15683 (1996).

[62] H.-L. Gross and W. Mader, Chem. Commun. (1) 55-56 Jan 7 (1997).

[63] B. Ollivier, R. Retoux, P. Lacorre, D. Massiot, and G. Férey, J. Mater. Chem. **7**, 1049 (1997).

[64] Y. Yourdshahyan, C. Ruberto, M. Halvarsson, L. Bengtsson, V. Langer, B. I. Lundqvist, S. Ruppi, and U. Rolander, Journal of the American Ceramic Society, feature article **82**, 1365 (1999).

[65] L. Smrčok, V. Langer, M. Halvarsson, and S. Ruppi, (2000), submitted to Z. Kristallogr.

[66] C. Ruberto, Y. Yourdshahyan, and B. I. Lundqvist, to be published.

[67] S. I. Simak, U. Haussermann, R. Ahuja, S. Lidin, and B. Johansson, Phys. Rev. Lett. **85**,

142 (2000).

[68] L. B. Hansen, K. Stokbro, B. I. Lundqvist, and D. M. Deaven, Phys. Rev. Lett. **75**, 4444 (1995).

[69] J. Hartford, B. von Sydow, G. Wahnström, and B. Lundqvist, Phys. Rev. B **58**, 2487 (1998).

[70] B. von Sydow, J. Hartford, and G. Wahnström, Computational Materials Science **15**, 367 (1999).

[71] J. Hartford, Phys. Rev. B **61**, 2221 (2000).

[72] S. V. Dudiy, J. Hartford, and B. I. Lundqvist, Phys. Rev. Lett. **85**, 1898 (2000).

[73] S. V. Dudiy, first-Principles Density-Functional Computational Experiments to Understand the Nature of Metal-Carbonitride Interface Adhesion, licentiate thesis, Göteborg University (2000).

[74] K. Carling, G. Wahnström, T. R. Mattsson, A. E. Mattsson, N. Sandberg, and G. Grimvall, Phys. Rev. Lett. **85**, 3862 (2000).

[75] E. Schröder, Phys. Rev. E **62**, 8830 (2000).

[76] A. D. Becke, Phys. Rev. A **30**, 3098 (1988).

[77] J. P. Perdew, K. Burke, and M. Ernzerhof, Phys. Rev. Lett. **77**, 3865 (1996).

[78] B. I. Lundqvist, Y. Andersson, H. Shao, S. Chan, and D. C. Langreth, Int. J. Quantum. Chem **56**, 247 (1995).

[79] Y. Andersson, D. C. Langreth, and B. I. Lundqvist, Phys. Rev. Lett. **76**, 102 (1996).

[80] E. Hult, Y. Andersson, B. I. Lundqvist, and D. C. Langreth, Phys. Rev. Lett. **77**, 2029 (1996).

[81] J. F. Dobson and B. P. Dinte, Phys. Rev. Lett. **76**, 1780 (1996).

[82] W. Kohn, Y. Meir, and D. E. Makarov, Phys. Rev. Lett. **80**, 4153 (1998).

[83] E. Hult, H. Rydberg, B. I. Lundqvist, and D. C. Langreth, Phys. Rev. B **59**, 4708 (1998).

[84] K. Rapcewicz and N. W. Ashcroft, Phys. Rev. B **44**, 4032 (1991).

[85] Y. Andersson and H. Rydberg, Physica Scripta **60**, 211 (1999).

[86] E. Hult and A. Kiejna, Surf. Sci. **383**, 88 (1997).

[87] Y. Andersson, E. Hult, P. Apell, D. C. Langreth, and B. I. Lundqvist, Solid State Commun. **106**, 235 (1998).

[88] E. Hult, P. Hyldgaar, B. I. Lundqvist, Phys. Rev. B, *in print* (2001).

[89] J. F. Dobson and J. Wang, Phys. Rev. Lett. **82**, 2123 (1998).

[90] H. Rydberg, B. I. Lundqvist, D. C. Langreth, and M. Dion, Phys. Rev. B **62**, 6997 (2000).

[91] E. Zaremba and W. Kohn, Phys. Rev. B **13**, 2270 (1976).

[92] H. Rydberg, P. Hyldgaard, N. Jacobsson, and B. I. Lundqvist, to be published.

[93] D. C. Langreth and S. H. Vosko, Phys. Rev. Lett. **59**, 497 (1987).

[94] N. D. Lang and W. Kohn, Phys. Rev. B **1**, 4555 (1970).

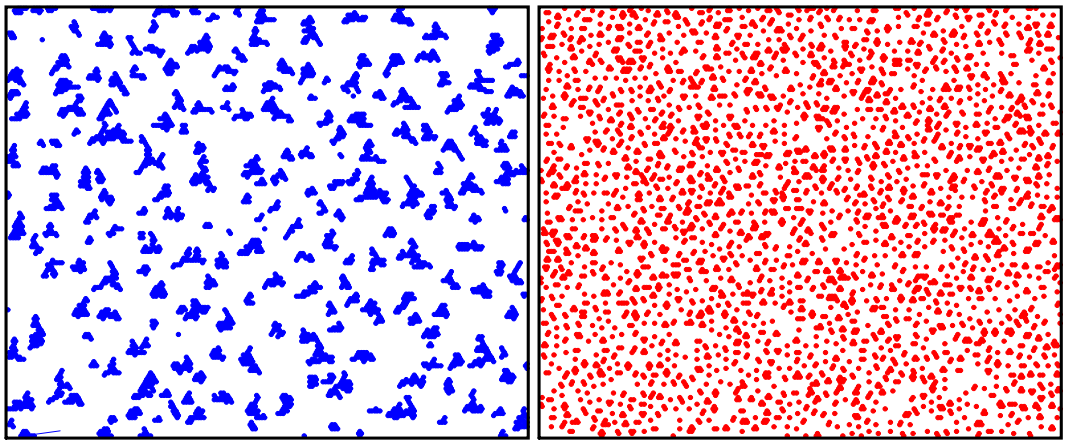

FIG. 1. Results of kinetic Monte-Carlo simulations for low-temperature island nucleation in homoepitaxial growth on Al(111) with (right) and without (left) interactions between the adatoms.[35]

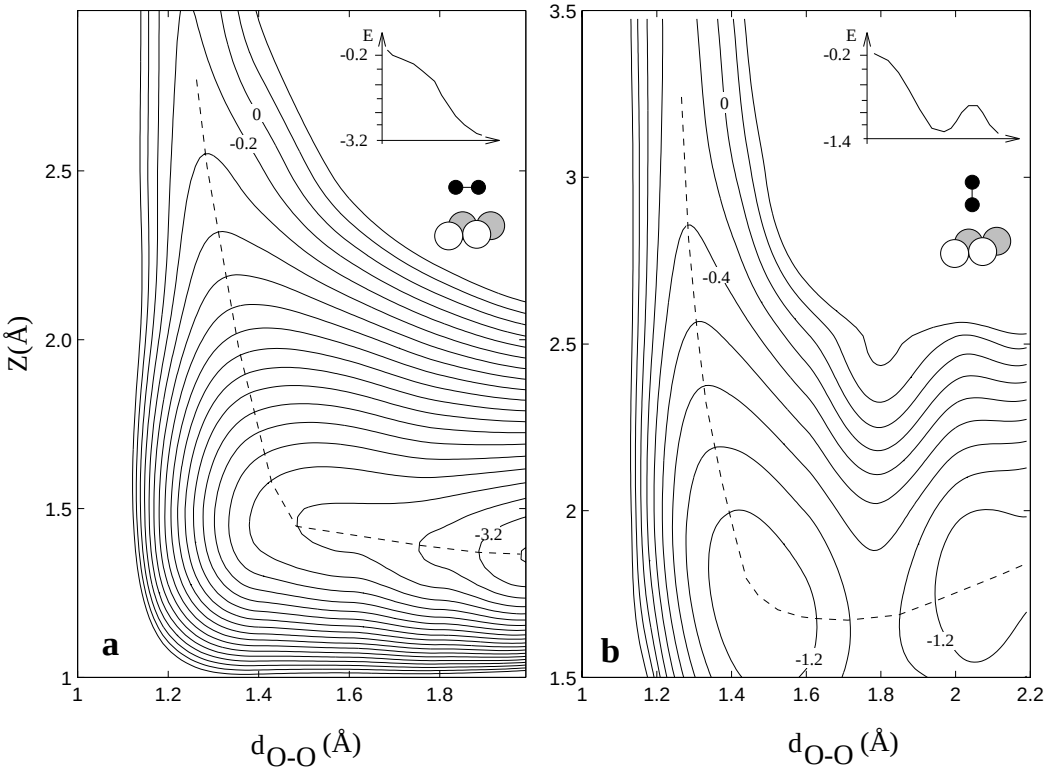

FIG. 2. Cuts through the six-dimensional PES of O_2 with bond length $d_{\mathrm{O-O}}$, a distance Z above the Al(111) surface on fcc site. The molecule-surface angles θ are (a) 90° and (b) 0°. The numbers in the equipotential contours are the energy values in eV measured from the energy of totally separated O_2 and Al(111) surface.[53]

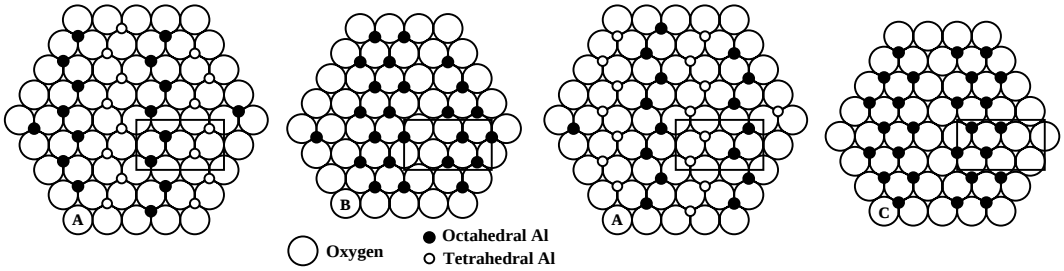

FIG. 3. The calculated bulk structure of κ-Al_2O_3 shown layer by layer (from left to right: O layers A, B, A, and C with Al overlayers, respectively). The stacking direction is [001]. Large open circles represent oxygen ions, while small circles show the aluminum ions in octahedral (filled circles) and tetrahedral (open circles) positions. The unit cell is drawn with solid lines in each layer.[64]

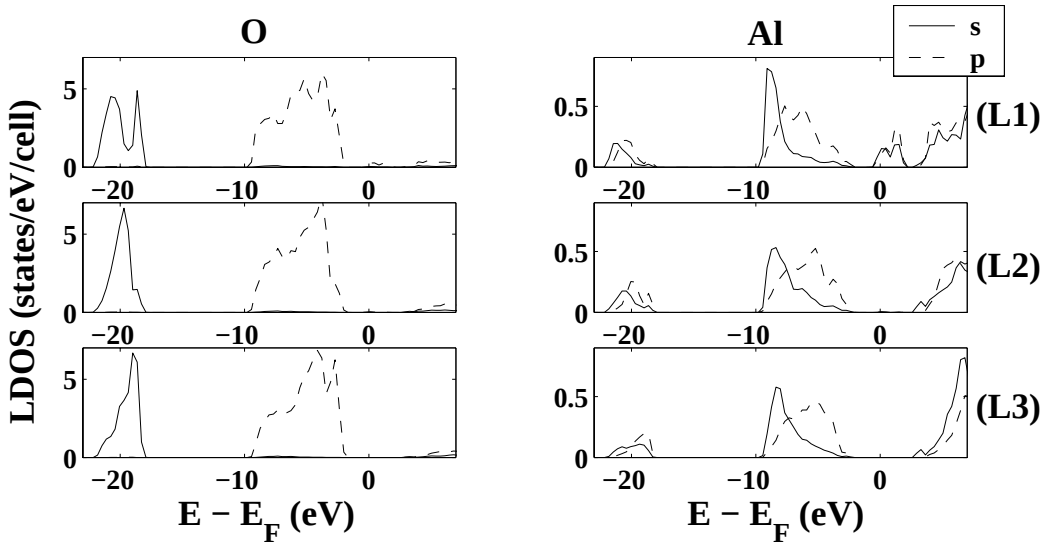

FIG. 4. Calculated local density of states (LDOS), projected onto s and p atomic orbitals, for the top three layers ("L1"–"L3") of the relaxed κ-$Al_2O_3(00\overline{1})$ surface.[66]

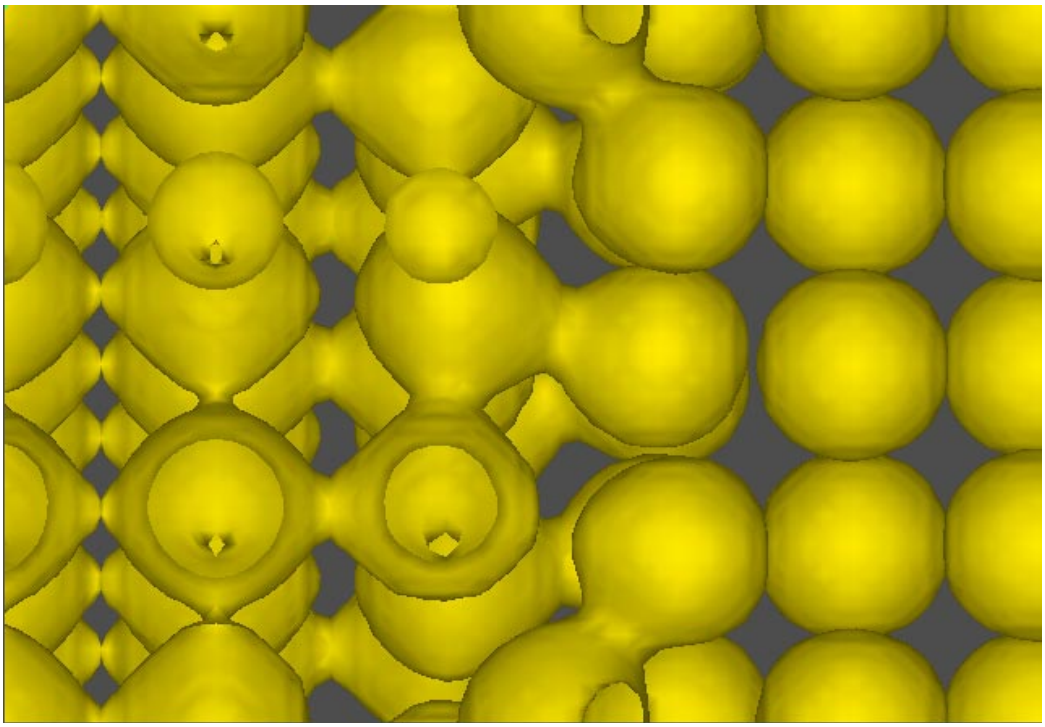

FIG. 5. Electron-density picture of bonding at the Co/TiC interface: Constant-density surface at the level of 0.5 electrons/Å^3.[72]

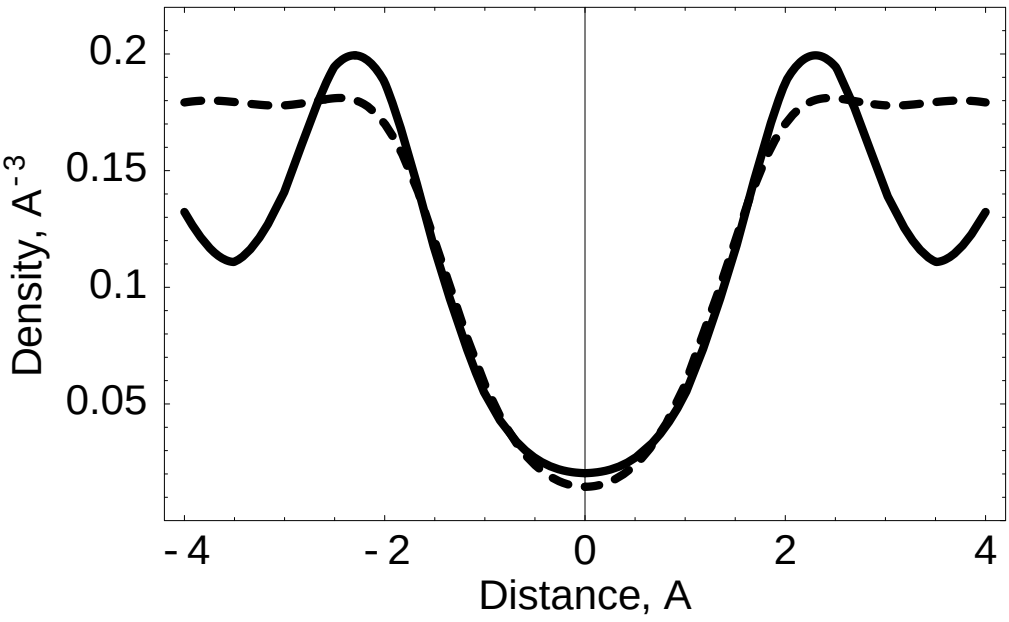

FIG. 6. The electron density in the <111> direction across a vacancy.[74] Solid line: density profile from DFT calculations. Dashed line: superimposed density profile from two juxtapositioned jellium surfaces,[94] 2.4 Å apart.

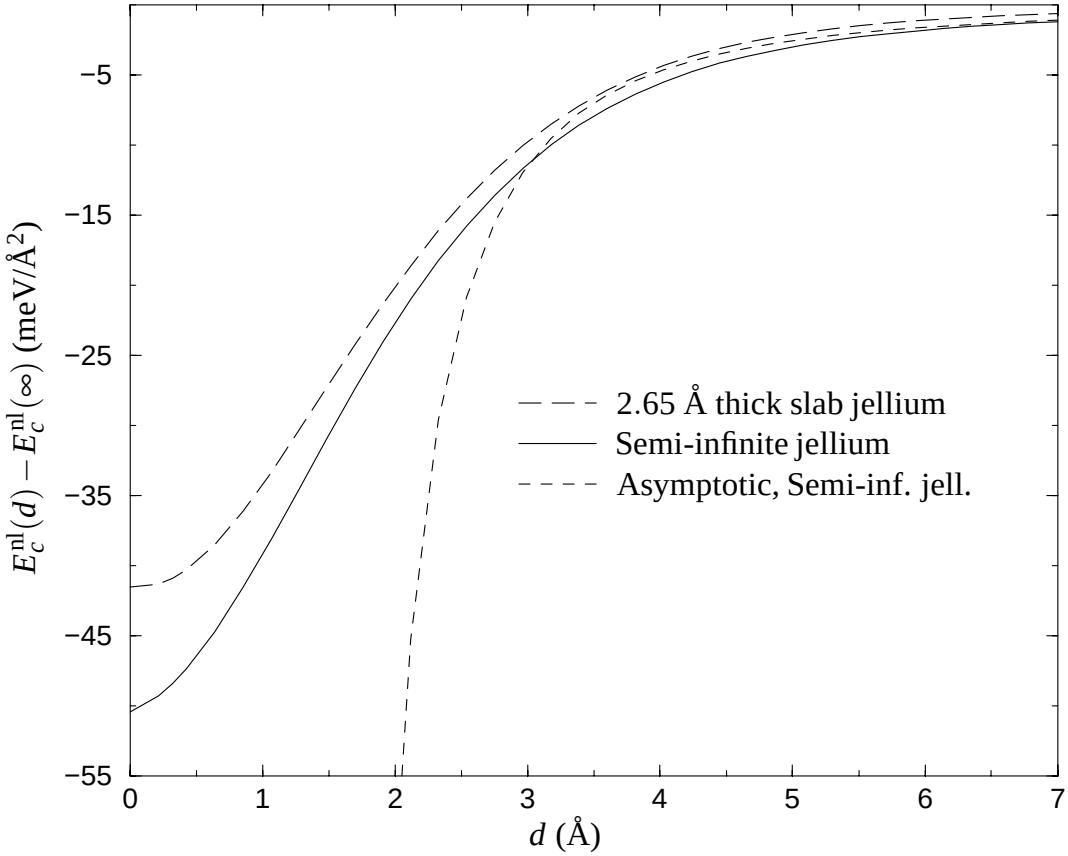

FIG. 7. Small-separation (d) variation of the non-local correlation-interaction energy between two semi-infinite jellia of $r_s = 2$.[90] Solid line: Linear superposition of self-consistent LDA density (SCLK). Dotted line: $E = -C_2/(d - 2Z_0)^2$, with $C_2 = 2.39\mu$Ha and $Z_0 = 0.96$ a.u.[87]